

Available online at <http://arjournal.org>

APPLIED RESEARCH JOURNAL

RESEARCH ARTICLE



ISSN: 2423-4796

Applied Research Journal

Vol.1, Issue, 2, pp.91-96, April, 2015

## EFFECT OF Mg SUBSTITUTED ON PHYSICAL AND MAGNETIC PROPERTIES OF Cu-Mg FERRITES

<sup>1</sup>M. A. Hakim, <sup>2\*</sup> Shahida Akhter, <sup>2</sup>D. P. Paul and <sup>3</sup>S. M. Hoque

<sup>1</sup>Dept. of Glass and Ceramic Engineering, Bangladesh University of Engineering and Technology, Dhaka.

<sup>2</sup>Department of Physics, University of Chittagong, Chittagong-4331, Bangladesh.

<sup>3</sup>Materials Science Division, Atomic Energy Centre, Dhaka-1000, Bangladesh.

### ARTICLE INFO

#### Article History:

Received: 19, March, 2015

Final Accepted: 20, April, 2015

Published Online: 25, April, 2015

#### Keywords:

Ferrites, XRD, Grain size, Magnetization, Magnetic moment.

### ABSTRACT

Polycrystalline  $\text{Cu}_{1-x}\text{Mg}_x\text{Fe}_2\text{O}_4$  ( $x=0.2, 0.4, 0.6, 0.8$  and  $1.0$ ) ferrites have been synthesized using solid-state reaction technique. Phase identification, morphology and magnetization measurements have been done by X-ray diffraction (XRD), Scanning Electron Microscope (SEM), VSM and SQUID magnetometer. Formation of the cubic spinel structure was observed by XRD studies. Grain size is found to decrease with increasing Mg content and increase with increasing sintering temperature. Field dependence of magnetization was measured at 300 K and 5 K using VSM and SQUID magnetometer. Saturation magnetization ( $M_s$ ) decreases with Mg content. The observed variation in  $M_s$  can be explained in terms of the cation redistribution between A and B sublattices. The substitution of Mg ions and effect of sintering temperature plays decisive role in changing structural and magnetic properties of Cu-Mg ferrites.

© Copy Right, ARJ, 2015. All rights reserved

## 1. INTRODUCTION

Ferrimagnetic cubic spinels, known as ferrites, possess properties of both magnetic materials and insulators and are important in many technological applications. Their structural, electrical and magnetic properties depend on magnetic interaction and cation distribution in the two sublattices, i.e., tetrahedral (A) and octahedral (B) sites. The study of spinel ferrites is of great importance from both the fundamental and the applied research point of view. They have many applications in high frequency devices and they play a useful role in technological and magnetic applications because of their high electrical resistivity and consequently for low losses over a wide range of frequency [1, 2]. The magnetic properties of the spinel ferrites are governed by the type of magnetic ions residing on the A- and B-sites and the relative strengths of the inter- $(J_{AB})$  and intra- $(J_{AA}, J_{BB})$  sublattice exchange interactions. When the A-B inter-sublattice interactions are much stronger than the A-A and B-B intra-sublattice interactions, the spins have a collinear structure in which moments on the moment on the B-sites. The advantages of the mixed spinel is that all interactions are well defined near-neighbour antiferromagnetic with  $|J_{AB}| \gg |J_{BB}| \gg |J_{AA}|$ .

Among all ferrites, Copper ferrite ( $\text{CuFe}_2\text{O}_4$ ) is one of the most important ferrites which has both magnetic and semiconducting properties and have widely used in electronic industry [3]. Mg-substituted ferrites have applications in transformer, ferro-fluids, magnetic cores of coils, catalysts, gas sensors and humidity sensors [4-6]. Extensive works has been reported regarding the non-magnetic substitution in the different ferrites system in order to improve their magnetic properties. The present work focused on change

\*Corresponding author: **Shahida Akhter**, Email: [shahida212@yahoo.com](mailto:shahida212@yahoo.com)  
Department of Physics, University of Chittagong, Chittagong-4331, Bangladesh.

of structural, microstructural and magnetization properties by the substitution of non-magnetic Mg in Cu-Mg ferrites.

## 2. MATERIAL AND METHODS

Ferrite samples of the chemical formula  $\text{Cu}_{1-x}\text{Mg}_x\text{Fe}_2\text{O}_4$  ( $x = 0.2, 0.4, 0.6, 0.8$  and  $1.0$ ) were prepared by the double sintering ceramic technique. High purity reagent nano-powders of CuO, MgO, and  $\text{Fe}_2\text{O}_3$  were mixed according to their molecular weight and mixed for 4 hours using agate mortar and pestle. Then the mixture was ball milled for 4 hours and the slurry was dried and was pressed into disc shape sample. The disc shaped sample was pre-sintered at  $1000^\circ\text{C}$  for 4 hours to form ferrite through chemical reaction. The pre-sintered material was again crushed and wet milled for another 4 hours in distilled water to reduce it to small crystallites of uniform size. The mixture was dried and a few drops of saturated solution of polyvinyl alcohol were added as a binder. The resulting powders were pressed uniaxially under a pressure of (20 Pa) in a stainless steel dies to make pellets. The pressed pellets were then finally sintered at  $1150^\circ\text{C}$  and  $1200^\circ\text{C}$  for 2 hours respectively in air and cooled in the furnace. All samples were heated slowly in the programmable Muffle furnace (Model HTL 10/17, Germany) at the rate of about  $220^\circ/\text{hours}$  increase to avoid cracking of the samples.

The crystal structure of the samples was identified using Phillips (PW3040) X' Pert PRO X-ray diffractometer with  $\text{CuK}_\alpha$  ( $\lambda=1.5406 \text{ \AA}$ ) radiation operated at 40kV and 30mA in the range of  $20\text{-}70^\circ$  with sample pitch of  $0.02^\circ$  at time for each step data collection was 1.0s at room temperature. Scanning Electron Microscope (SEM) (Model: FEI Inspect S50) was employed to examine the microstructural features such as grain size. Before taking the micrographs, the surfaces of the samples were thermally etched at a temperature of  $150^\circ\text{C}$  below their sintering temperatures. The grain size was determined by linear intercept method from surface micrographs of samples. To measure the magnetization behavior of the prepared samples, the field dependence of magnetization has been measured at 300K by using Vibrating Sample Magnetometer (VSM) (Model EV7) at Materials Science Division, Atomic Energy Centre, Dhaka, Bangladesh and at 5K by SQUID (MPXL5) Magnetometer at Ågstrom Laboratory, Uppsala University, Sweden.

## 3. RESULTS AND DISCUSSION

### 3.1. XRD pattern

The crystal structure identification and lattice constant determination was performed on an X-ray diffraction pattern (XRD). Typical XRD pattern for all samples of the system  $\text{Cu}_{1-x}\text{Mg}_x\text{Fe}_2\text{O}_4$  ferrites sintered at  $1200^\circ\text{C}$  for 2 hr is illustrated in Figure 1. The data showed intense sharp peaks and reveal well-crystalline single phase spinel structure for all Mg content. No other crystalline phase was observed indicating good stability of the ferrite compositions. Analysis of these patterns shows that the sample has a cubic structure. It is obvious that the characteristics peaks for spinel Cu-Mg ferrites appear in the samples as the main crystalline phase. The peaks (220), (311), (222), (400), (422), (511) and (440) correspond to spinel phase.

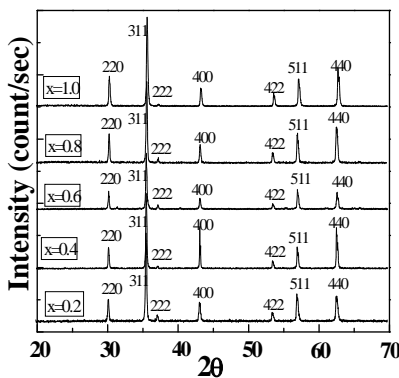


Figure 1 XRD pattern of Cu-Mg ferrites for  $x=0.4$ .

### 3.2. Lattice parameter

The lattice parameter refers to the constant distance between the unit cell in a crystal lattice. The lattice constant was determined through the Nelson-Riley extrapolation method. The values of the lattice constant

obtained from each reflected plane are plotted against Nelson-Riley function [7]:  $F(\theta) = \frac{1}{2}[\cos^2\theta/\sin\theta + \cos^2\theta/\theta]$ , where  $\theta$  is the Bragg's angle and straight lines are obtained. The accurate values of lattice constant were estimated from the extrapolation of these lines to  $F(\theta)=0$  or  $\theta=90^\circ$ . The value of lattice parameter 'a' was found 8.389, 8.384, 8.378, 8.372 and 8.365 Å for Mg content  $x=0.2, 0.4, 0.6, 0.8$  and  $1.0$  respectively. It is noticed that the value of lattice parameter 'a' decreases with the increasing Mg content and follows Vegard's law [8]. This variation can be explained on the basis of an ionic size difference of the component ions. This is evident due to the substitution of small ionic radius  $Mg^{2+}$  (0.66 Å) ions on the expense of larger  $Cu^{2+}$  (0.73 Å) ions [9]. This causes a decrease in size of the unit cell, where the length of the edge of unit cell decreases from 8.389 to 8.365 Å.

### 3.3. Micrographs

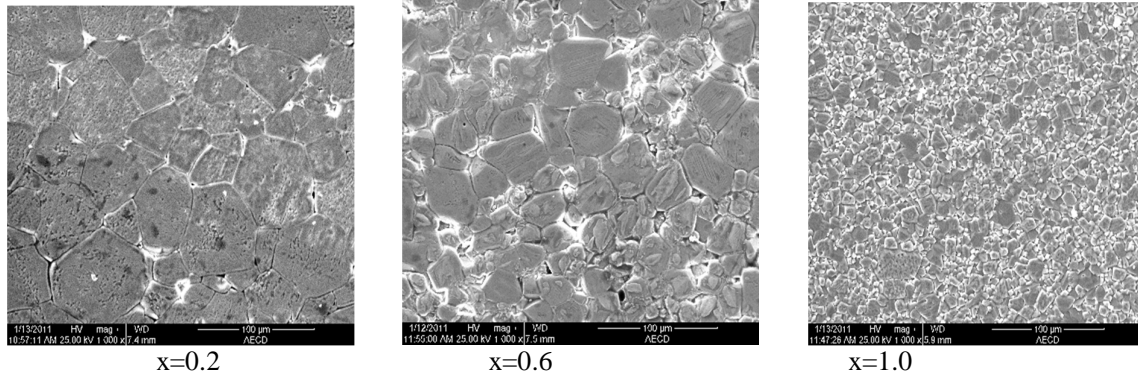


**Figure 2** SEM micrographs for  $x=0.2, 0.6, 1.0$  samples of  $Cu_{1-x}Mg_xFe_2O_4$  ferrites at  $T_s=1200^\circ C$ .

Figure 2 shows the cross-sectional Scanning Electron Microscopy (SEM) images of the Cu-Mg (for  $x=0.2, 0.6$  and  $1.0$ ) ferrites sintered at  $1200^\circ C$ . It is observed from above Figures that rounder grains are visible which indicating signs of the onset of intra-granular 'honeycombing'. The grain growth mechanism is compromised between driving force for grain boundary movement and retarding force of pores and inclusion during the sintering process [10]. During the sintering, the thermal energy generates a force that drives the grain boundaries to grow over pores. Thereby decreasing the pore volume and making the material dense. When the driving force of the grain boundary in each grain is homogeneous, the sintered body attains a uniform grain size distribution.

### 3.4. Grain Size

The average grain sizes of the samples was calculated using the line intercept method from the SEM micrographs is illustrated in Figure 3 in which the average grain size decreases with increasing Mg content. The similar decreasing trend in grain size was also observed by N. Reslescu et. al. in Mg-Zn [11] and S. Akhter et. al. Li-Cd [12]. This is because MgO acts as a microstructural stabilizer responsible for finer and uniform grain size. Also MgO is a stable oxide avoids presence of divalent iron and there by circumvent tendency of discontinuous grain growth. Moreover the decrease of grain size could be due to increase of intra-granular porosity since the pores neutralize the driving force and the thickness of the grain boundary is found to increase with a decrease in grain size.

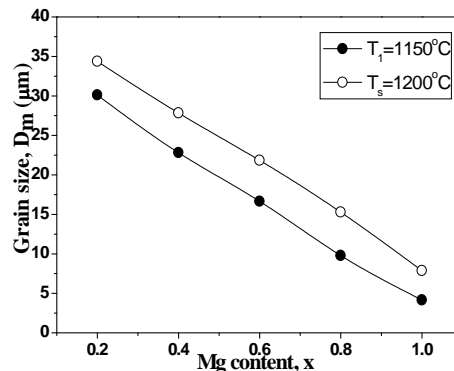


**Figure 3** Variation grain size,  $D$  ( $\mu m$ ) with Mg content ( $x$ ) at different  $T_s$ .

### 3.4. Magnetization Study

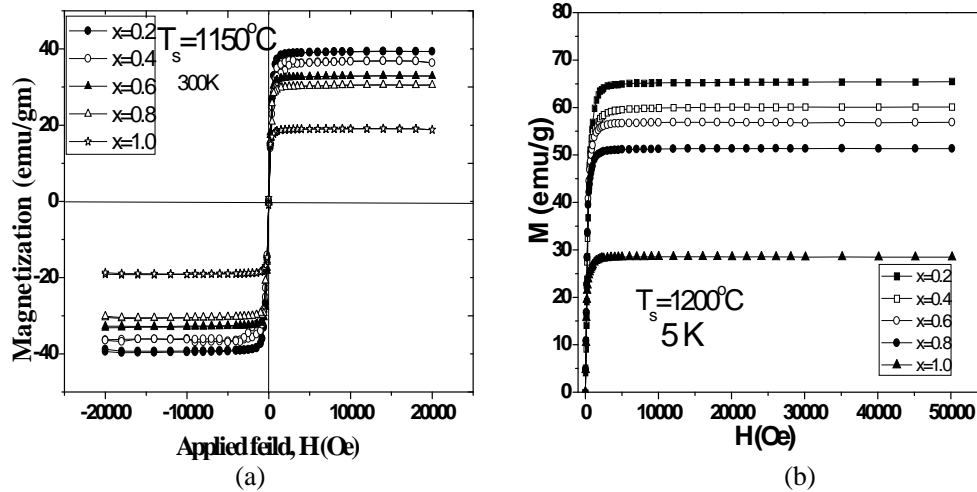


Figure 4 Field dependence magnetization at (a) 300K by VSM and (b) 5K by SQUID.

The magnetization measurement of the  $\text{Cu}_{1-x}\text{Mg}_x\text{Fe}_2\text{O}_4$  series was measured by using VSM at 300K and SQUID at 5K and has been presented in Fig. 4. Figures show the typical characteristics of superparamagnetic behavior like the absence of hysteresis, almost immeasurable coercivity [13]. All the samples exhibit very low coercivity values indicating that all the samples belong to the family of soft ferrites. The magnetization of all samples increases linearly with increasing applied magnetic field up to 0.1 T. Beyond this applied field the magnetization attains maximum values and then saturation occurs.

### 3.5. Saturation Magnetization

The saturation magnetization ( $M_s$ ) has been obtained by extrapolation of  $M$  vs  $\frac{1}{H}$  to  $1/H \rightarrow 0$  and presented in Figure 5 at 5K. From Fig, it is observed that as the Mg content increase the saturation magnetization decrease with the value 58.5 to 27.36 emu/g and 65.12 to 28.53 emu/g at 5K for 1150°C and 1200°C. Similar decrease of  $M_s$  with  $x$  content is observed in Ni-Mg by Akhter [14] and in Mg-Zn by Rajesh [15]. In general  $\text{Mg}^{2+}$  ion have their strong preference for B sites and a very few have preference to occupy A-sites where as  $\text{Cu}^{2+}$  have usual preference to occupy B-sites [16]. The preference of  $\text{Mg}^{2+}$  ions into the B-sites will encourage migration of  $\text{Fe}^{3+}$  ion into A-site causing increasing magnetization of A-site while that of B-site magnetization decreases. From Fig. 6, it is also observed that  $M_s$  increases with increasing sintering temperature from 1150°C to 1200°C. It is observed that grain size increase with  $T_s$ . The magnetization caused by domain wall movement requires less energy than that requires by domain rotation. It is easy for the domain wall movement to magnetize or demagnetize the samples with larger grain size. Samples with larger grain are expected to have high  $M_s$  with higher  $T_s$ .

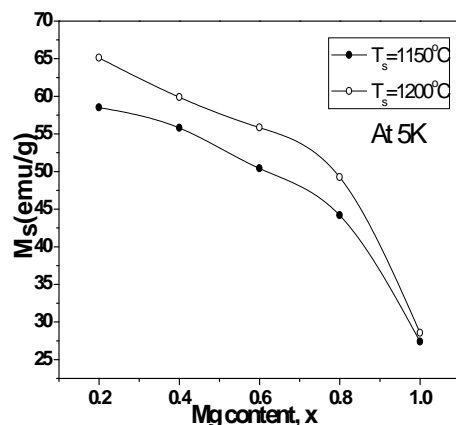


Figure 5 Variation of  $M_s$  with Mg content at 5K.

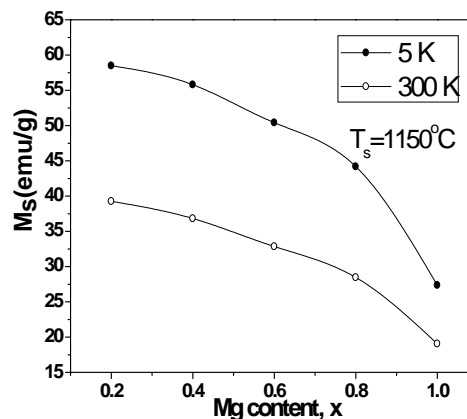


Figure 6  $M_s$  at 300K and 5K for  $T_s=1150^\circ\text{C}$ .

The variation of  $M_s$  with Mg content at 300K & 5K is shown in Figure 6. It is observed that  $M_s$  decrease with increase of temperature due to the thermal vibration of spin magnetic moment of the ferrite at higher temperature. The  $M_s$  increase with decrease in temperature can be explained by a linear equation and it is known as the Bloch's law [17]:  $M_s(T) = M_s(0)[1 - BT^{3/2} - CT^{5/2}]$  where  $M_s(0)$  the  $M_s$  extrapolated at 0k, B and C are constants and  $M_s(T)$  the  $M_s$  at T K. At low temperature spin frustration is decreased and the spin alignment due to applied external magnetic field (H).

#### 4. CONCLUSION

The polycrystalline  $\text{Cu}_{1-x}\text{Mg}_x\text{Fe}_2\text{O}_4$  ( $x=0.2$  to 1.0 with step 0.2) ferrites have been prepared by conventional double sintering ceramic techniques sintered at 1150<sup>o</sup>C and 1200<sup>o</sup>C for 2 hrs. The effect of Mg substituted in Cu-Mg ferrites was investigated and the following observations have been found:

1. The X-ray diffraction pattern reveals the confirmation of single phase cubic spinel structure of all the ferrites. By increasing the Mg content the lattice parameters decreased as a result of the smaller ionic radius of  $\text{Mg}^{2+}$  as compared to  $\text{Cu}^{2+}$  ion.
2. The sintering temperature and non-magnetic Mg substitution have a great influence on the average grain size. The average grain size decrease with increasing Mg content whereas increase with increasing sintering temperature.
3. From magnetization as a function of applied magnetic field  $M(H)$ , it is clear that all samples are soft ferrites because of very low coercivity. The magnetization increases sharply at low field and become saturated with increasing applied magnetic field.
4. The saturation magnetization decreases linearly with increase in Mg substitution which has been explained by the cation distribution and exchange interaction, since the distribution of cation in A and B sites influence the magnetic properties of ferrites.
5. The value of  $M_s$  increases with decreasing temperature. This behavior implies the co-existence of ferromagnetic and anti-ferromagnetic interactions. The decrease in  $M_s$  at higher temperature may be due to the super-paramagnetic response of individual magnetic clusters that can be ferromagnetic or ferromagnetic in nature.

#### 5. ACKNOWLEDGEMENT

The author (Shahida Akhter) grateful to Materials Science Division of Atomic Energy Centre, Dhaka, Bangladesh for allowing her prepare the samples and to utilize its laboratory facilities and Ångström Laboratory, Solid State Division, Uppsala University, Sweden for doing at low temperature measurements by SQUID.

#### 6. REFERENCES

- [1] Sugimoto M. 1999. The past, present and future of ferrites. *J. Am. Ceram. Soc.* 82: 269-280.
- [2] Watawe S.C., Bamne U.A., Gonbare S.P. and Tangsali R.B. 2007. Preparation and dielectric properties of cadmium substituted lithium ferrite using microwave-induced combustion. *Mater. Chem. Phys.* 103: 323-328.
- [3] Darul J. and Nowicki W. 2009. Preparation and neutron diffraction study of polycrystalline Cu-Zn-Fe materials. *Radiat. Phys. Chem.* 78: S109-111.
- [4] Chen Q. and Zhang Z.J. 1998. Size-dependent superparamagnetic properties of  $\text{MgFe}_2\text{O}_4$  spinel ferrite nanocrystallites. *Appl. Phys. Lett.* 73: 3156-3158.
- [5] Benko F.A. and Koffyberg E.P. 1986. The effect of defects on some photo-electrochemical properties of semiconducting  $\text{MgFe}_2\text{O}_4$ . *Mater. Res. Bull.* 21: 1183-1188.
- [6] Tinashu Z. Hing P. Jianheng Z. and Kingbing K. 1999. Ethanol-sensing characteristics of cadmium ferrite prepared by chemical coprecipitation. *Mater. Chem. Phys.* 61: 192-198.
- [7] Cullity B.D. 1959. Elements of X-ray diffraction. Addison-Wesley, M.A. 329-330.
- [8] Whinfry C.G. Echart D.W. and Tauber A. 1960. Preparation and X-Ray Diffraction Data<sup>1</sup> for Some Rare Earth Stannates. *J. of Am. Chem. Soc.* 82(11): 2695-2997
- [9] Bhosale D.N. Sawant S.R. Gangal S.A. Mahajan R.R. and Bakare P.P. 1999. Synthesis of copper-magnesium-zinc ferrites and correlation of magnetic properties with microstructure. *Mater. Sci. Eng. B* 65(20): 79-89.
- [10] Pujar, R.B. Bellad S.S. Watawe S.C. Chougule B.K. 1999. Magnetic properties and microstructure of  $\text{Zr}^{4+}$ -substituted Mg-Zn ferrites. *Mater. Chem. Phys.* 57: 264.

- [11] Rezlescu N. Rezlescu E. Pasnicu C. Craus M.L. 1994. Effects of the rare-earth ions on some properties of a nickel-zinc ferrite J. Phys.: Condns. Matter 6: 5707
- [12] Akhter S. Paul D.P. Hakim M.A. Hoque S.M. 2011. Microstructure and Electromagnetic Properties of Li-Cd Ferrites. Proc. of Inter. Conf. of Magnetic Materials (ICMM-2010). 1347: 244-247.
- [13] Herzer G. 1990. Grain Size Dependence of Circuity and Permeability in Nanocrystalline Ferromagnets. IEEE Trans. Magn. 26: 1397.
- [14] Akhter Hossain A.K.M. Biswas T.S. Takeshi Yanagida. Hidekazu Tanka. Histoshi Tabata. Tomoji Kawai. 2010. Investigation of Structural and Magnetic Properties of Polycrystalline  $\text{Ni}_{0.50}\text{Zn}_{0.50-x}\text{Mg}_x\text{Fe}_2\text{O}_4$ . Mater. Chem. Phys. 120: 461-467.
- [15] Rajesh Lyer. Rucha Desai and Upadhyay R.V. 2009. Low temperature synthesis of nanosized  $\text{Mn}_{1-x}\text{Zn}_x\text{Fe}_2\text{O}_4$  ferrites and their characterizations. Bull. Mater. Sci. 32(2): 141-147.
- [16] Gobal M.A. 2009. Effect of Mg substitution on the magnetic properties of NiCuZn ferrite nanoparticles prepared through a novel method using egg white. J. Magn. Mater. 321: 3144.
- [17] Bloch F. 1930. Zur Theorie des Ferromagnetismus Z. Phys. 61: 206.